Journal of Applied Sciences

ISSN 1812-5654

science alert

ANSInet
an open access publisher
http://ansinet.com

Journal of Applied Sciences 10 (7): 526-534, 2010
ISSN 1812-5654

Petrography and Geochemical Signatures in Cracks Filling Calcite Sequences in Septarian Concretions, Sanganeh Formation, Kopet-Dagh Basin, NE Iran

[1]A. Mahboubi, [1]R. Moussavi-Harami, [2]L.B. Collins and [3]J.R. Muhling
[1]Department of Geology, Ferdowsi University of Mashhad, Mashhad, Iran
[2]Department of Applied Geology, Curtin University of Technology, Perth, Western Australia
[3]Centre for Microscopy Characterization and Analysis, University of Western Australia,
35 Striling Highway, Crawley, Perth, W. Australia

Abstract: The objectives of this study were to understand the stages of crack-fill calcite in these concretions that can help in a better understanding of these secondary structures in NE Iran as well as other parts of the world. Petrography and stable isotopes signatures revealed that the septarian concretions are multiphase and display several stages of cementation (G_2 to G_4). The earliest carbonate matrix (septarian body, called G_1) with $\delta^{13}C$ and $\delta^{18}O$ values of 0.01 and -21‰ PDB, respectively, precipitated from seawater during shallow burial and anaerobic microbial oxidation of organic matter. The formation temperature of G_1 is calculated to be 15.5° C. The Presence of authigenic pyrite with G_1 supports the interpreted environment of precipitation. Calcite from the walls to the central parts of the cracks (G_2 to G_4) showed increasing crystal sizes, clarity and depletion of $\delta^{18}O$ values. The formation temperature of G_4 is calculated to be 54°C. The $\delta^{13}C$ values in three generations of calcite showed no major differences. These data revealed that the cracks are filled by calcite during burial, which the last generation formed at higher temperatures than the temperature of the nodules.

Key words: Kopet-dagh, NE Iran, septarian concretion, carbon isotope, oxygen isotope

INTRODUCTION

In general, septarian concretions are ovoid and spheroid shape with various diameters. They have mainly display more or less regular cracks (Hudson *et al*., 2001; Seilacher, 2001). These cracks have been hypothesized by shrinkage of the center of rather a soft or hardened shell, by expansion of gasses produced during bacterial decay of organic matter or by brittle fracturing of a rigid concretion nucleus during compaction (Astin and Scotchman, 1988) or earthquakes (Pratt, 2001). In shale, dehydration of gel-rich (Aso *et al*., 1992), or soap-rich centers (Criss *et al*., 1988) have been proposed. The cracks are usually filled, completely or partially by one or more generation minerals such as carbonate and sulphates.

The fillings of cracks are even more diverse, because they record events which took place either soon after the concretion body formed, or long afterward and record a history of precipitation episodes (Hudson *et al*., 2001).

The concretion growth mechanisms have been reviewed by Raiswell and Fisher (2000). Most early studies assumed that concretion grow concentrically outwards, starting from a point of nucleation, but some researcher such as Coleman and Raiswell (1993, 1995) believed that they can grow by pervasive cementation of a body of sediment of essentially the same size as the ultimate concretion (Mozley, 1989).

Although, there are numerous publications on septarian concretions in all parts of the world (e.g., Mozley, 1989; Coniglio *et al*., 2000; Raiswell and Fisher, 2000; Pratt, 2001; Hendry *et al*., 2006; Melezhik *et al*., 2007) but, this is the first time that these secondary sedimentary structures will be considered in Iran and compared with other septarian concretions.

Petrography and geochemical analysis of these sedimentary structures are very useful indicators of carbon source and pore-fluid types during concretion growth and can be used to monitor changes in the interstitial pore waters of the sediment as the concretion grew and, in the case of septaria, cracked and became filled with later mineral growths.

This study is focused on septarian concretions of Sanganeh Formation in Easternmost part of the Kopet-Dagh Basin in NE Iran (Fig. 1). This intracontinental basin was formed in Northeast Iran and Southwestern Turkmenistan after closure of the Hercynian Ocean following the Middle Triassic Orogeny

Corresponding Author: Mahboubi Asadollah, Department of Geology, Ferdowsi University of Mashhad, Mashhad, Iran
Tel/Fax: +98 511 8797275

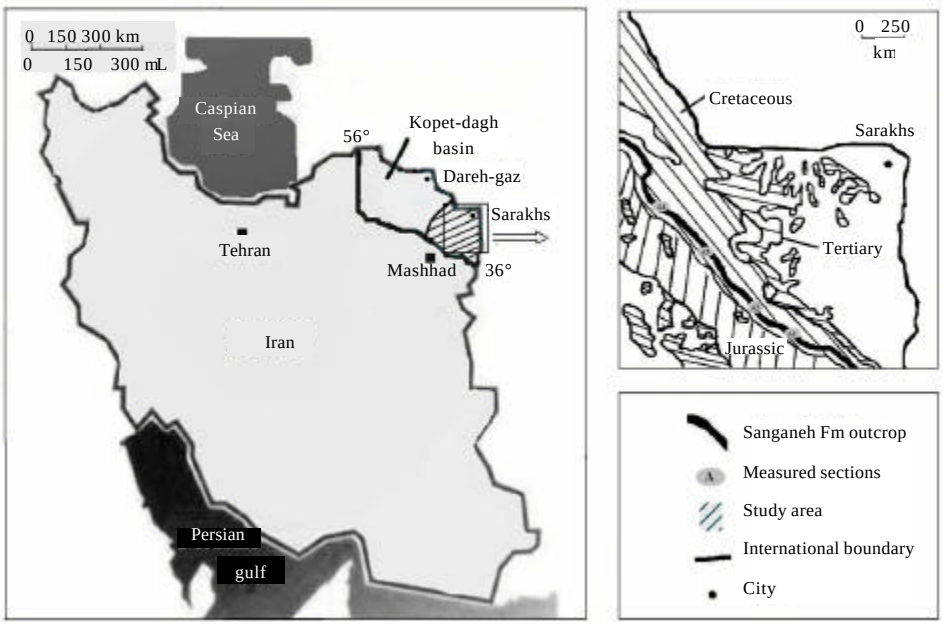

Fig. 1: Location map of studied area

(Berberian and King, 1981; Rutnner, 1991, 1993; Alavi *et al*., 1997). The thickness of sediments in the Eastern portion of this Basin is nearly 8 km (Moussavi-Harami and Brenner, 1992; Afshar-Harb, 1994) and in Turkmenistan may have reached up to 15 km (Lyberis *et al*., 1998). Sanganeh formation is deposited during upper cretaceous (Albian) time and may have been deposited in relative low energy conditions in outer shelf. It is mainly composed of dark grey to black shale with minor amounts of thin siltstone and fine-grained sandstone interbeds. The thickness of this formation at type locality (in Kalat-Naderi road Northwest of Sanganeh village) is about 740 m (Afshar-Harb, 1994). One of the most common features in this formation, is the presence of various secondary sedimentary structures such as cone in cone, nodules and especially septarian concretion.

Sanganeh Formation in all localities in eastern parts of the Kopet-Dagh basin is divided into 3 parts (Afshar-Harb, 1994) (Fig. 2). Lower part is composed of alternation of silty shale with fine-grained sandstone and siltstone. Middle part consists of dark to black shale and upper part is composed of green to grey shale. Septarian concretions occurred in middle part with high abundance. These structures exhibit characteristics including predominantly calcitic composition, various sizes (from 10 cm to 1 m in diameter and the width/height ratio lower than 1.3), commonly subspherical to oblate spheroidal shape, polygonal and radiating pattern of cracks with no preferred orientation, with widest cracks in the concretion margins and narrowing towards the centre of the concretions and finally multiple generations of cement-filling cracks (Fig. 3A-C).

This study will be done based on sedimentological data, petrographic observations of cracks filling calcites and their geochemical analysis for interpretation of various types of fluids during calcite precipitation. A combination of textural and geochemical information affords the best opportunity to record the evolution of abiotic and biogeochemical processes in this type of concretion (e.g., Desrochers and Al-Aasm, 1993; Hudson *et al*., 2001).

MATERIALS AND METHODS

For this study, all outcrops of sanganeh formation from type locality toward the eastern parts of the Kopet-Dagh basin (Fig. 1) have been visited during August 2007. More than 40 concretions were collected from various localities for the study area. These samples had 15 to 70 cm in diameters. Two hundred thin sections have prepared from these samples in various directions, in the Department of Geology, Ferdowsi University of Mashhad Iran, for better understanding of crystal shapes of carbonate septa in concretions. Most thin sections have stained by Alizarin Red S for separation of calcite

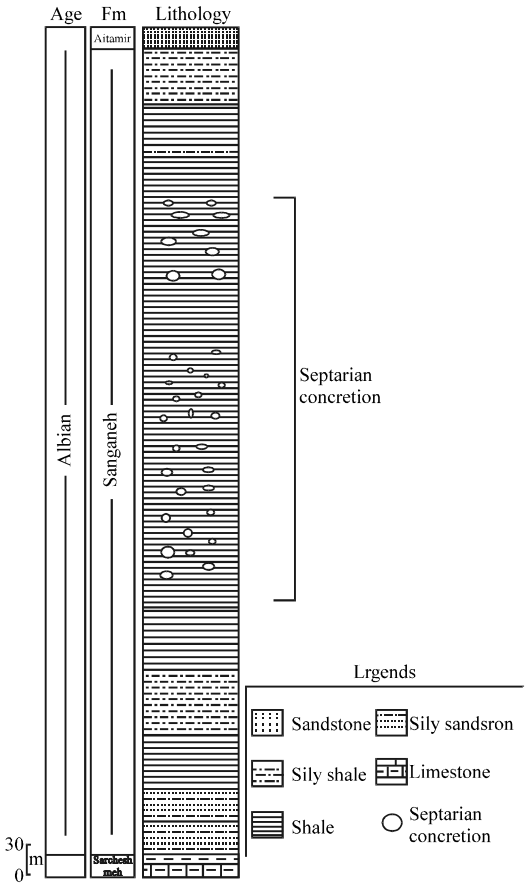

Fig. 2: Simplified stratigraphic column of sanganeh formation at type locality showing location of septarian concretions

from dolomite as well as Potassium Ferricyanide solution for Fe bearing minerals based on Dickson (1965). We also examined all polished thin sections by cathodoluminescence microscopy using a Technosyn Cold CL (Model 8200 Mk3) at 12 KV and 160- 195 μA with an automatic camera in sedimentology Lab. in Geology Department at Ferdowsi University of Mashhad. Based on petrographic studies, 20 points in different parts of cracks filling calcites were selected for carbon and oxygen analysis. A microscope-mounted dental drill with 500 μm bit was used to extract calcite powder from polished slab. About, 0.2 mg of each sample was reacted with anhydrous phosphoric acid in individual reaction vessels in a vacuum at 72°C. The CO_2 extracted from each sample was analyzed by isotope ratio mass spectrometry. Analytical error of carbon and oxygen isotopes is ±0.1 per mil. Both, carbon and oxygen isotopes values are reported relative to PDB standard. EDS analysis for carbonate collected on JEOL JSM 6400 SEM with Oxford instruments Link Analytical EDS detector at 15 kv and 5 nA beam current. Data reduction has done using Isis software. Standards including Fe metal (Fe), Mn metal (Mn), Periclase (Mg), Wollastonite (Ca,Si), Celestine (Sr), Corundum (Al) and Apatite (P). WDS analysis for Barite and Apatite collected on a JEOL JSM6400 SEM fitted with 3 wavelength dispersive spectrometers at 15 kv and 20 nA beam current. Data reduction with Moran Scientific software and standards as above plus Albite (Na), Orthoclase (K), Barite (Ba), Celestine (S), Nacl (Cl) and Apatite (F). All of the analytical analysis, were done in the Centre for Microscopy Characterization in the University of Western Australia, during the first author sabbatical leave in 2009.

RESULTS

Data from the calcite filling cracks in studied septarian concretions, such as mineralogy as well as carbon and oxygen isotope values. Stable isotopes analysis and cross-plot of these data are one of the best ways to recognize the various generation of calcite vein-filling, therefore these cross-plot are shown in Fig. 4. Based on these data (crystal shape and stable isotope values), four distinctive stages of calcite formation are recognized in septarian concretion, referred to as G_1 to G_4 in ascending order. These stages can be related to various generation types

G_1 is the first calcite type, with clay to silt size crystal (Fig. 5A) and dark brown color (Fig. 5B-D). They are predominantly non ferroan as well as non-luminescent. Dissolution of this type of calcite in HCl acid (10%) showed that G_1 has near 24% insoluble residue. These are including clay minerals, quartz in silt size and pyrite. In general, G_1 has formed the main parts of septarian concretion body in studied samples. Cross cutting of G_1 by G_2 indicates that ongoing cracking is continued during early cementation. Oxygen and carbon isotope values range from 0.01 and -21‰ PDB, respectively.

G_2 is the second type calcite and earliest cement that precipitated follows G_1 with relatively elongated to bladed shapes crystals (length to wide ratio is more than 3), moderately inclusion, ferroan (Fig. 3D, A) and non-luminescent. These cements form the thickest parts and optically continuous and show the prominent sweeping extinction indicative of fascicular optic calcite. Calcite crystal sizes are gradually increase toward internal parts of cracks and modified to equant shape. Carbon and oxygen isotope values of G_2 range from -18.21 to -17.57 and -2.85 to -0.71‰ PDB, respectively.

G_3 has lighter oxygen isotope values than later types and ranges from -4.25 to -7.17‰ PDB. Carbon isotope

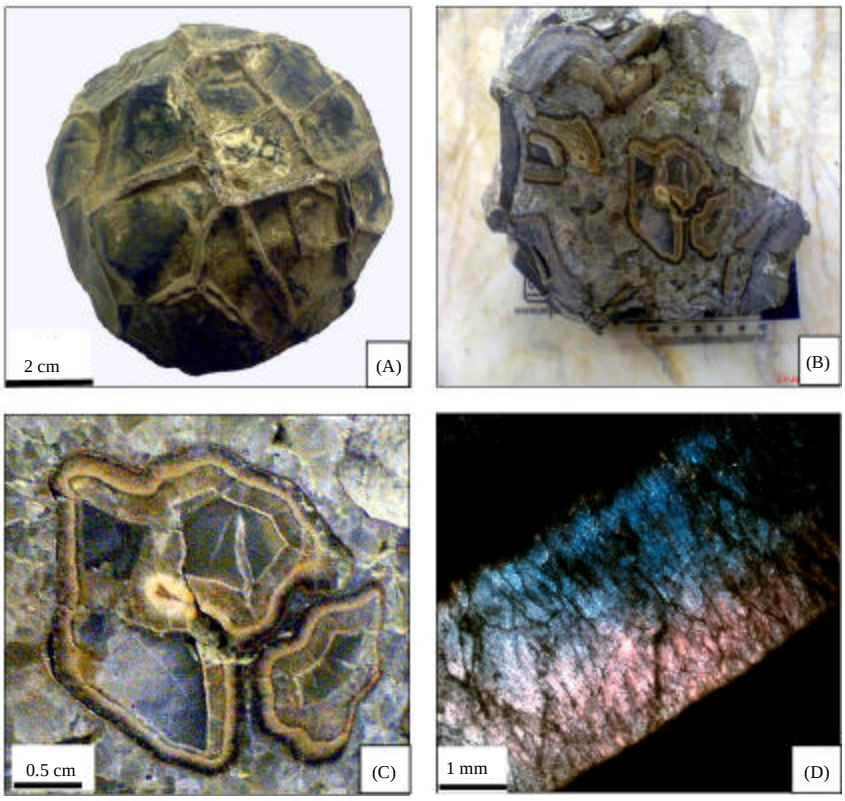

Fig. 3: Examples of Sanganeh concretions. (A) A photograph of septarian concretion showing calcite filling cracks, (B) Polished slab of a calcite septarian concretion with radial and concentric cracks filled by various fabric and color of calcite. Minor residual porosity is also seen, (C) close up with details of polished concretion slab of photo B and (D) photomicrograph of stained thin section (PPL) showing zoned septarian crack with subsequent ferroan (blue) and non-ferroan (red) calcite

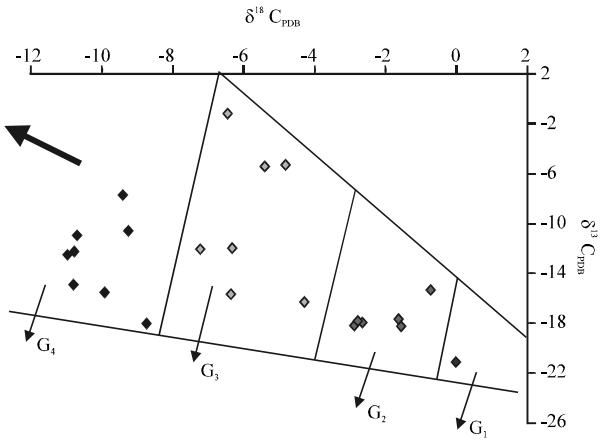

Fig. 4: Scatter diagram δ^{18} O vs. δ^{13} C showing four generation G_1 to G_4 of septarian concretions in studied area. Large arrow shows filling direction of wall to centre in cracks

values ranges from -1.20 to -16.19‰ PDB. These calcites crystals are larger size than G_1 and G_2 as well as length to wide ratio changes and are relatively to be close together. They are more clearly and relatively inclusion free, nonferroan and non-luminescent. Calcite extinction is similar to G_2 (Fig. 5A).

G_4 has the lightest values of oxygen isotopes and ranges from -8.70 to -10.94‰ PDB, while the carbon isotope values are about -7.72 to -18.01‰ PDB. G_4 is filled central parts of cracks with clear crystal and, blocky and equant fabrics (Fig. 5A). The largest crystal sizes are present here and mean size ranges from 0.5 to 1.2 mm (Fig. 5A). In some cracks, these cements have not completely filled pore spaces and a minor porosity (intercrystaline type) has been remained. G4 is nonferoan, non-luminescent as well as free of inclusion.

It is noted that WDS analysis (Table 1, Fig. 6A, B) showed that in some samples, cracks are lined with barite crystals and disseminated apatite.

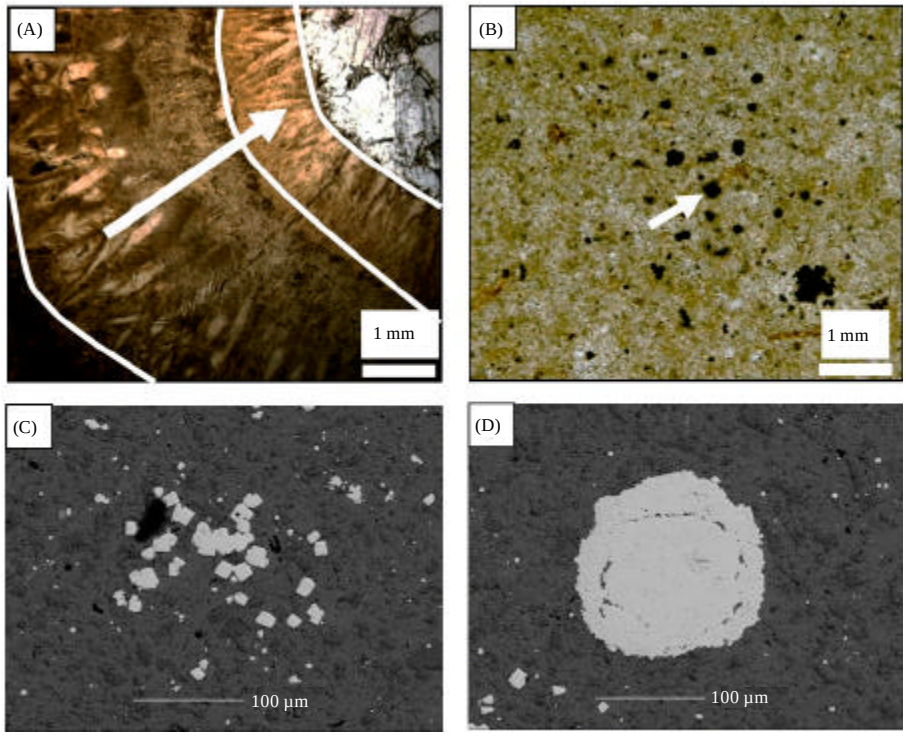

Fig. 5: (A) Cross-polarized view of thin section photomicrograph of septarian cements showing G1 to G4 generations (in arrow direction) with relatively sharp boundary. Noted to different size and fabrics of calcite crystals that have various carbon and oxygen isotope values (see text). Scale bar is 1 mm. (B) Close-up view of G_1 photomicrograph showing micron size calcite contains authigenic pyrite (white arrow). Scale bar is 0.1 mm. (C) SEM view of euhedral pyrite in G_1. (D) Close up of one frambiodal pyrite in SEM view

Table 1: EDS and WDS analysis of calcite, barite and apatite cracks filling in septarian concretions of studied area

Calcite samples No.	1	4	6	7	8	9	11	12	13	14	16	17	18
$FeCO_3$	0.00	1.32	1.29	1.55	1.61	2.10	1.82	1.74	1.31	1.23	1.21	1.76	1.90
$MnCO_3$	0.00	0.44	1.13	1.20	0.91	0.96	0.94	0.81	0.84	1.31	1.23	0.55	1.31
$MgCO_3$	5.23	3.22	0.69	0.79	0.75	0.86	1.05	0.90	0.86	0.00	0.73	1.15	1.07
$CaCO_3$	92.96	84.32	96.05	93.00	97.05	94.94	93.69	95.82	99.51	99.64	97.46	96.34	95.64
$SrCO_3$	0.00	0.00	0.00	0.00	0.00	0.00	0.00	0.00	0.00	0.00	0.00	0.00	0.00
SiO_2	0.86	8.81	0.00	0.00	0.00	0.00	0.00	0.00	0.00	0.00	0.00	0.00	0.00
Al_2O_3	0.42	2.34	0.00	0.00	0.00	0.00	0.00	0.00	0.00	0.00	0.00	0.00	0.00
P_2O_5	0.30	0.00	0.00	0.00	0.16	0.23	0.25	0.00	0.14	0.00	0.14	0.21	0.23
Total	99.77	100.45	99.16	96.54	100.48	99.09	97.75	99.27	102.66	102.18	100.77	100.01	100.15

Barite samples No.	36	38	39	50	51	Apatite sample No.	45
SiO_2	0.02	0.01	0.02	0.01	0.01	$SiO2$	0.00
Al_2O_3	0.11	0.13	0.12	0.11	0.14	Al_2O_3	0.00
FeO	0.00	0.00	0.00	0.00	0.00	FeO	0.02
MnO	0.00	0.00	0.00	0.00	0.00	MnO	0.00
MgO	0.01	0.02	0.00	0.00	0.01	MgO	0.01
CaO	0.06	0.08	0.07	0.03	0.10	CaO	55.60
Na_2O	0.12	0.13	0.13	0.15	0.14	Na_2O	0.00
K_2O	0.00	0.00	0.03	0.01	0.02	K_2O	0.01
BaO	67.22	66.95	67.15	67.25	67.73	BaO	0.10
SrO	0.18	0.27	0.17	0.19	0.22	SrO	0.00
P_2O_5	0.03	0.05	0.06	0.04	0.07	P_2O_5	40.06
SO_3	32.93	32.90	31.58	32.58	32.43	SO_3	0.08
Cl	0.00	0.04	0.00	0.00	0.00	Cl	0.02
F	0.00	0.03	0.00	0.00	0.00	F	4.43
Total	100.68	100.61	99.33	100.38	100.87	Total	100.33

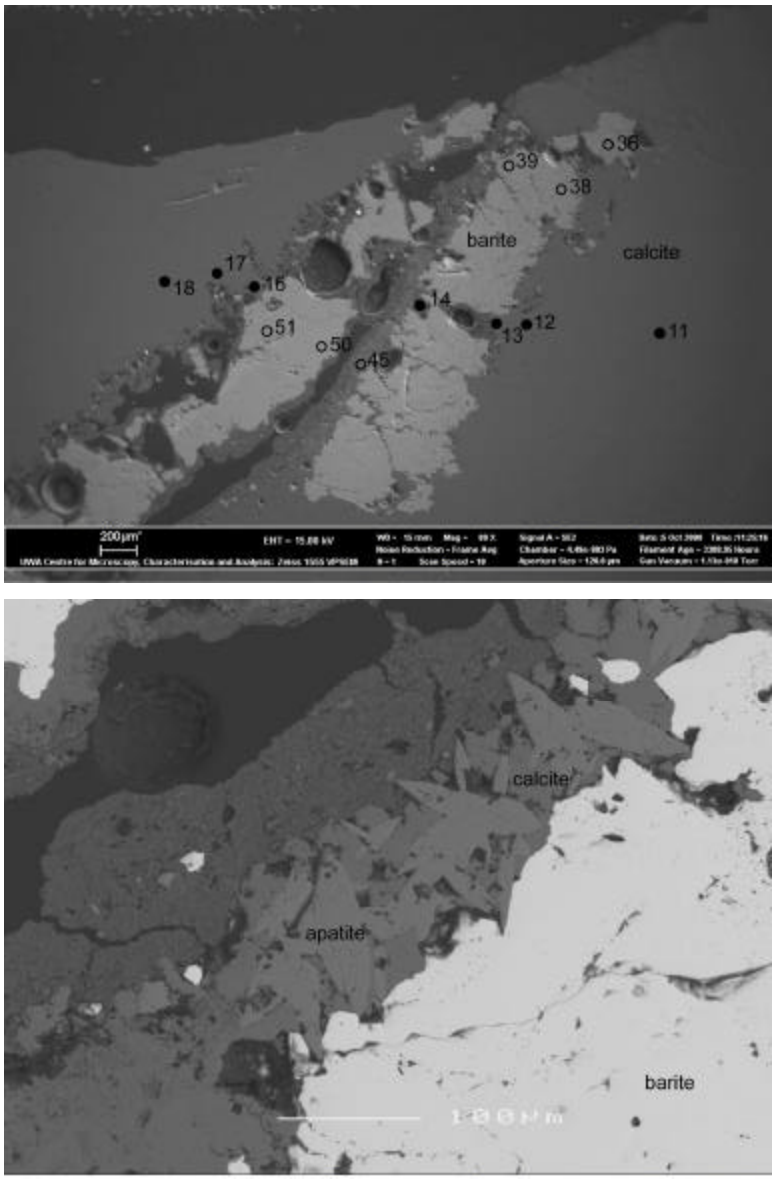

Fig. 6: (A) SEM photo that shows number and location of EDS and WDS analysis. (B) Back scatter photo of cracks filling show calcite, apatite and barite formation

DISCUSSION

As may be expected, there is a broad spectrum of carbon and oxygen isotopes values in analyzed samples ($\delta^{13}C$ ranges from -21.00 to -1.20‰ PDB and $\delta^{18}O$ ranges from -10.94 to 0.01‰ PDB). This indicates that sanganeh concretions in studied area are multiphase and display several stages of cementation. Carbon isotope composition varies widely in sedimentary environments (Morse and Mackenzie, 1990) and is a function of the initial sedimentary organic carbon pool modified by the mechanisms of its decomposition (Hudson, 1977). Photosynthesis, decomposition by biochemical or mineral oxidation during burial as well as bacterial sulfate reduction in marine sediments always can lead to $\delta^{13}C$ depletion in organic matter, typically in the range of -12 to -25‰ (Hudson, 1977; Anderson and Arthur, 1983). Diagenetic carbonates may also contain mixed of all carbon isotope values (Mozley and Burns, 1993).

Seawater oxygen isotope composition is geological time dependent. It has probably remained in the range of -2 to 0‰ from the Late Jurassic to present, although , it

may have been much lower in earlier oceans water (Lecuyer and Allemand, 1999). Temperature, carbonate mineralogy and infiltration of meteoric waters into strata of marine origin can lead to crystallization of minerals with strongly negative $\delta^{18}O$ values (Hudson *et al*., 2001).

G_1 with lightest carbon isotope value (-21‰ PDB) and finest crystal size may have formed under shallow burial conditions during the anaerobic microbial oxidation of organic matter (e.g., Coleman, 1993). These calcites due to much depletion in carbon isotope, nonferroan composition as well as presence of authigenic pyrite may have precipitated in sulfate reduction condition during shallow burial. G_1 has very Low iron or non ferroan (pink with ARS) because, iron is mainly removed and combined with HS to form authigenic pyrite (e.g., Coleman, 1993). It is very similar to what have been interpreted by Coniglio *et al*. (2000) from Cretaceous septarian concretions of Pueblo in Colorado, USA.

G_2 is the first larger and elongate crystals that filled major parts of cracks in studied septarian concretions. Cement morphology (elongated and bladed with more than 3:1 in L: W ratio) showed that this calcite generation is precipitated from fluid with high flow rate, high Mg/Ca ratios and HCO_3^{-2} supply (Given and Wilkinson, 1985) that can be similar to sea water composition. Blue color in stained thin sections as well as non-luminescence reflection is also revealed that this fluid may have contained Fe^{2+} and has filled cracks during reduction condition but Mn^{2+} values have been lower than amounts that can led to high brightness in CL (e.g., Budd *et al*., 2000). The range of oxygen isotope of studied samples (-2.85 to -0.71‰ PDB) can support the interpretation that G_2 precipitated by sea water because this value is similar to oxygen isotope composition that was reported by Lecuyer and Allemand (1999) for Late Jurassic time and before. Carbon isotope value is relative heavier than G_1 but reflects that the source of carbon for this type should have been similar to G_1 and form from the degradation of organic matter in sulfate reducing condition (e.g., Mozley and Burns, 1993).

G_3 is the thickest part of crack filling calcite and has widely range of carbon (-1.20 to -16.19‰ PDB) and narrow range of oxygen (-4.25 to -7.17‰ PDB) isotopes values. Wide range indicates that the carbon in calcite was provided from both decay of organic matter and the dissolved inorganic carbon of residual seawater. The relatively light oxygen isotopes in this calcite suggested that they have formed where, the pore water still retained the residual sea water composition. Presence of non-ferroan and non luminescent calcite showed that G_3 may have precipitated during oxidation environments.

G_4 with lightest value of oxygen isotope (-8.70 to -10.94‰ PDB) with clear, blocky and equant fabric shows high depletion of oxygen isotopes. It can be done by many factors including influx meteoric water, interaction between sea water and sediments particularly with reactive volcanic materials, upwelling of hot fluids, increasing temperature and recrystallization of early carbonate cement during deep burial (Morad *et al*., 1996). Because, there is no evidence of volcanic activity in the Kopet-Dagh basin (Afshar-Harb, 1994), it seems that temperature increases during burial is the best answer for decreasing oxygen isotope values.

The carbon isotope values of G_4 are similar to previous calcite types and much depleted (range between -7.72 to -18.01‰ PDB). It suggested that the carbon pool for all calcite types has been the same and should have been from degradation of organic matter in sulfate reducing environment (e.g., Mozley and Burns, 1993). Different degrees and wide range of depletion can be reflected the amount of organic matter available. Woo and Khim (2006), interpreted that these range of carbon isotopes in carbonate concretions of the Miocene Yeonil Group in the Pohang Basin of Korea can be due to combination of organic parts and unalterated coexisting of mollusks.

In some cracks, the last generation of mineralization is barite that cut calcites. Although, its origin vary quite widely (Hudson *et al*., 2001), but it seems Barium may has been in main body of concretion (G_1) and supported from underlying paleo-aquifer. Another source of sulphate can be from residual sea water sulphate after substantial sulphate reduction.

As earlier stated, although several mechanisms have been presented to describe crack formation, but dehydration (synaresis) and shrinkage is apparently the most popular mechanism for studied concretion. The time of this process can be during early diagenesis at a shallow burial depth and prior to significant compaction. The approximately spherical shapes of most concretions is also supported this hypothesis, otherwise, they would have caused most concretions to be more flattened in forms. Since, there is no similarity in direction of bedding fractures and concretion cracks; therefore they are unlikely to be tectonic cracks.

For calculation of temperature of the fluids from which, the G_1 was precipitated, we used Anderson and Arthur's (1983) Eq. 1 as follows:

$$T = 16.0-4.14\,(\delta c-\delta w) + 0.13(\delta c-\delta w)^2 \quad (1)$$

where, T is temperature, δc is the oxygen isotope value of calcite relative to PDB and δw is the oxygen isotope value of water relative to SMOW.

By using the least-altered calcite, $\delta^{18}O$ values of -0.01‰ and -1.2‰ for oxygen isotope value for after Late Jurassic time, the calculated temperature is about 15.5°C. It showed fluid temperature during formation of septarian concretion within Sanganeh. By using -8.70‰ for highest value of oxygen isotope of G_4, the calculated temperature is about 54° C that showed minimum temperature of fluid for last generation (G_4) of calcite formation during deeper burial and higher temperature than G_1.

CONCLUSION

Sanganeh formation (Albian) in Eastern Kopet-Dagh Basin, NE Iran, has many septarian concretions. These are mainly present in middle part of this formation with various sizes and multistage crack filling calcite. Main bodies of these concretions (G_1) form from clay to silt size grain, non ferroan, non-luminescent carbonate and dark brown color with authigenic pyrite. Oxygen and carbon isotopes in G_1 are heaviest and lightest, respectively. G_1 may have formed under shallow burial conditions during the anaerobic microbial oxidation of organic matter from sea water fluids. It seemed that cracks are formed during shrinkage and are mainly filled by calcite. G_2 is the earliest and G_4 is the latest calcite filling phase in concretion cracks with increasing crystal sizes from wall toward the center of the cracks. Concretion paragenetic analysis based on calcite fabrics as well as carbon and oxygen isotopes values showed a multistage formation of calcite in G_2 to G_4 from shallow to deeper burial conditions. Calculated temperature for G_1 and G_4 are 15.5 and 54°C, respectively.

ACKNOWLEDGMENT

Authors gratefully acknowledge from Ferdowsi University of Mashhad, Faculty of Science, Iran for financial supporting of this project (grant No.: p/1019-3rd December 2008).

REFERENCES

Afshar-Harb, A., 1994. Geology of the Kopet-Dagh. Published by Geological Survey of Iran, Tehran, pp: 265.

Alavi, M., H. Vaziri, K. Seyed-Emami and Y. Lasemi, 1997. The triassic and associated rocks of the Aghdarband area in central and north eastern Iran as remnant of the southern Turanian active continental margin. Geol. Soc. Am. Bull., 109: 1563-1575.

Anderson, T.F. and M.A. Arthur, 1983. Stable Isotopes of Oxygen and Carbon and Their Application to Sedimentologic and Paleoenvironmental Problems. In: Stable Isotopes in Sedimentary Geology, Arthur, M.A., T.F. Anderson, I.R. Kaplan, J. Veizer and L. Land (Eds.). SEPM, Georgia, pp: 1-151.

Aso, E., T.J. Gisbert and B.V. Garces, 1992. Type septaria-cone in cone nodules in the Stephano-Permian of the Catalan Pyrenees. Carbonates Evaporites, 7: 132-139.

Astin, T.R. and I.C. Scotchman, 1988. The diagenetic history of some septarian concretions from the Kimmeridge Clay, England. Sedimentology, 35: 349-368.

Berberian, M. and G.C.P. King, 1981. Toward a paleogeographic and tectonic evolution of Iran. Can. J. Earth Sci., 18: 210-265.

Budd, D.A., U. Hammes and B.W. Ward, 2000. Cathodoluminescence in calcite cements: New insights on Pb and Zn sensitizing, Mn activation and Fe quenching at low trace-element concentrations. J. Sedimentary Res., 70: 217-226.

Coleman, M.L., 1993. Microbial processes: Controls on the shape and composition of carbonate concretions. Mar. Geol., 113: 127-140.

Coleman, M.L. and R. Raiswell, 1993. Microbial mineralization of origin of organic matter: Mechanisms of self-organization and inferred rates of precipitation of diagenetic minerals. Philosophical Trans. Phys. Sci. Eng., 344: 69-87.

Coleman, M.L. and R. Raiswell, 1995. Source of carbonate and origin of zonation in pyri tiferous carbonate concretions: Evaluation of dynamic model. Am. J. Sci., 295: 282-308.

Coniglio, M., P. Myrow and T. White, 2000. Stable carbon and oxygen isotope evidence of cretaceous sea-level fluctuations recorded in septarian concretions from Pueblo, Colorado, USA. J. Sedimentary Res., 70: 700-714.

Criss, R.E., G.A. Cooke and S.D. Day, 1988. An organic origin for the carbonate concretions of the Ohio shale. US. Geol Survey Bull., 1836: 21-21.

Desrochers, A. and I. Al-Aasm, 1993. The formation of septarian concretions in Queen Charlotte Islands, B.C.: Evidence for microbially and hydrothermally mediated reactions at shallow burial depth. J. Sedimentary Res., 63: 282-294.

Dickson, J.A.D., 1965. A modified staining technique for carbonate in thin section. Nature, 205: 287-287.

Given, R.K. and B.H. Wilkinson, 1985. Kinetic control of morphology, composition and mineralogy of abiotic sedimentary carbonates. J. Sedimentary Res., 55: 109-119.

Hendry, J.P., M.J. Pearson, N.H. Trewin and A.E. Fallick, 2006. Jurassic septarian concretions from NW Scotland record interdependent bacterial, physical and chemical processes of marine mudrock diagenesis. Sedimentology, 53: 537-565.

Hudson, J.D., 1977. Stable isotopes and limestone lithification. J. Geol. Soc. London, 133: 637-660.

Hudson, J.D., M.L. Coleman, B.A. Barreiro and N.T.J. Hollingworthes, 2001. Septarian concretions from the Oxford Clay (Jurassic, England, UK): Involvement of original marine and multiple external pore fluid. Sedimentology, 48: 507-531.

Lecuyer, C. and P. Allemand, 1999. Modelling of the oxygen isotope evolution of seawater: Implications for the climate interpretation of the 18O of marine sediments. Geochimica Cosmochimica Acta, 63: 351-361.

Lyberis, N., G. Manby, J.T. Poli, V. Kalugin, H. Yousouphocaev and T. Ashirov, 1998. Post triassic evolution of the southern margin of the Turan plate. Comptes Rendus l'Acad. Sci. Ser. IIA-Earth Planetary Sci., 326: 137-143.

Melezhik, V.A., A.E. Fallick, R.A. Smith and D.M. Rosse, 2007. Spherical and columnar, septarian, 18O-depleted, calcite concretions from middle-upper permian lacustrine siltstones in Northern Mozambique: Evidence for very early diagenesis and multiple fluids. Sedimentology, 54: 1389-1416.

Morad, S., L.F. de Ros and I.S. Al-Aasm, 1996. Origin of low 18O, pre-compactional ferroan carbonates in the marine Sto Formation (Middle Jurassic), offshore NW Norway. Mar. Pet. Geol. 13: 263-276.

Morse, J.W. and F.T. Machenzie, 1990. Geochemistry of Sedimentary Carbonates. Elsevier, New York, pp: 707.

Moussavi-Harami, R. and R.L. Brenner, 1992. Geohistory analysis and petroleum reservoir characteristics of Lower Cretaceous (Neocomian) sandstone, eastern portion of Kopet-Dagh Basin, northeast Iran. AAPG Bull., 76: 1200-1208.

Mozley, P.S., 1989. Complex compositional zonation in concretionary siderite: Implication for geochemical studies. J. Sedimentary Res., 59: 815-818.

Mozley, P.S. and S.J. Burns, 1993. Oxygen and carbon isotopic composition of marine carbonate concretions: An overview. J. Sedimentary Res., 63: 73-83.

Pratt, B.R., 2001. Septarian concretions: Internal cracking caused by synsedimentary earthquakes. Sedimentology, 48: 189-213.

Raiswell, R. and Q.J. Fisher, 2000. Mudrock-hosted carbonate concretions: A review of growth mechanisms and their influence on chemical and isotopic composition. J. Geol. Soc. London, 157: 239-251.

Rutnner, A.W., 1991. Geology of the Agh-Darband area (Kopet-Dagh, NE Iran): The Triassic of Agh-Darband, NE Iran and its pre-Triassic frame (Ed A/W. Rutnner). Abhandlung Geologische Bundes Anstalt, 38: 7-79.

Rutnner, A.W., 1993. Southern borderland of Triassic Laurasia in north-east Iran. Geologische Rundschau, 82: 110-120.

Seilacher, A., 2001. Concretion morphologies reflecting diagenetic and epigenetic pathways. Sedimentary Geol., 143: 41-57.

Woo K.S. and B.K. Khim, 2006. Stable oxygen and carbon isotopes of carbonate concretions of the Miocene Yeonil Group in the Pohang Basin, Korea: Types of concretions and formation condition. Sedimentary Geol., 183: 15-30.